sustainability

MDPI

Article

Biopolymers Produced by Treating Waste Brewer's Yeast with Active Sludge Bacteria: The Qualitative Analysis and Evaluation of the Potential for 3D Printing

Gregor Drago Zupančič [1,*], Anamarija Lončar [1], Sandra Budžaki [2] and Mario Panjičko [1]

[1] CROTEH Ltd., Avenija Dubrovnik 15, 10020 Zagreb, Croatia; anamarija.loncar@croteh.eu (A.L.); mario.panjicko@croteh.eu (M.P.)
[2] Faculty of Food Technology Osijek, Josip Juraj Strossmayer University of Osijek, Franje Kuhača 18, 31000 Osijek, Croatia; sandra.budzaki@ptfos.hr
* Correspondence: gregor.zupancic@croteh.eu

Abstract: Biopolymers are a suitable alternative for the ongoing problem of plastic accumulation, even though commercialization is difficult, which is reflected in the price of the product. However, costs can be reduced if active sludge bacteria and cheap, accessible substrates such as waste brewer's yeast are used. Waste brewer's yeast is a rich source of carbon and nitrogen and is widespread as a substrate in various industries. Thus, the cultivation of active sludge bacteria was performed on waste brewers' yeast to obtain biopolymers that can be used in 3D printing. FT-IR, TG, and DSC analyses of produced polymers were conducted after extraction, as well as biogas and biomethane potential tests. Results of cultivation under various conditions show that biopolymer content is extremely heterogeneous. However, during cultivation in SBR, signals at 1741.3, 1709.6, 1634.3, and 1238 cm^{-1} were detected. Further analyses are needed, but when said results are compared to those of consulted scientific articles, there is an indication that at least a small amount of PHA is present in biomass produced in SBR. Biopolymers produced in SBR were used as a material for the 3D printing of a cube. Moreover, testing of the physical properties (Young's modulus) of a 3D-printed cube was performed. After conducting experiments, it can be concluded that said process, although time-consuming, achieved the goal of printing a stable and rigid 3D-printed cube made from biopolymers. Further optimization of said process should focus on more detailed microbial selection as well as biopolymer extraction. In that way, isolation, purification, and identification techniques will be improved, which could achieve higher biopolymer yield and, thus, make biopolymers more accessible in various industries.

Keywords: brewers' yeast; active sludge bacteria; anaerobic digestion; biogas potential; biopolymer; 3D printing

Citation: Zupančič, G.D.; Lončar, A.; Budžaki, S.; Panjičko, M. Biopolymers Produced by Treating Waste Brewer's Yeast with Active Sludge Bacteria: The Qualitative Analysis and Evaluation of the Potential for 3D Printing. *Sustainability* **2022**, *14*, 9365. https://doi.org/10.3390/su14159365

Academic Editor: Sergi Maicas

Received: 12 June 2022
Accepted: 27 July 2022
Published: 30 July 2022

1. Introduction

Even though most manufacturers prioritise the production of durable and long-lived products, it is desirable for food packaging to have a precisely defined life cycle due to its purpose [1]. Biopolymers show great potential as packaging materials and are especially interesting due to their biodegradability. Biodegradable packaging material can have a variable chemical composition such as gelatine, starch, cellulose, and polylactide, while further trends in the food industry encourage the production of edible biofilm made from polysaccharides, proteins, and lipids [2]. When 3D printing is applied, packaging materials can be adjusted for special purposes, and biodegradable, raw, natural materials, such as dried *Mischanthus* and broken seashells, can be used as the raw material for 3D printing [1]. Furthermore, due to its properties, a suitable alternative to conventional plastics is bioplastics, especially in the agricultural, medical, and pharmaceutical industries [3].

Polyhydroxyalkanoates (PHA) are a type of biodegradable plastic that can be produced via a microbial process [4]. However, commercialization of bioplastics is difficult, which is reflected in the price of the product–one kg of bioplastics is at least three times more expensive than the one kg of traditional plastics [3]. The PHA production costs can be reduced if cheap and, above all, widespread and affordable substrates, such as renewable sources and agricultural waste, are used. Moreover, the use of cheaper microbial cultures such as activated sludge bacteria (because of their robustness and because they do not require aseptic conditions) contributes to the lower cost of produced biopolymers [5]. The results of the research by Andreasi Bassi et al. [6] confirm that PHA can successfully replace petroleum-derived polyurethane and that PHA obtained from the first generation of biomass (sugarcane and corn) has a significant impact on the environment and production costs–four times less impact on the environment and even up to eight times lower price than the mentioned polyurethane [6]. It has also been confirmed that from different, advanced generations of biomass (lignocellulosic-based residues) as a carbon source, different polyhydroxyalkanoate polymers with distinct polymer properties can be obtained. One of the carbon sources that has proven to be promising is waste brewers' yeast [7]. Many interesting biopolymers are produced by bacteria, since those that have studied production by yeast observed low biosynthesis yield [8]. The literature about the production of PHB using brewers' yeast is relatively scarce, but Ospina-Betancourth et al. [9] observed that a PHB concentration of 1.5 g/L can be achieved using wastewater from the yeast-production industry.

Polyhydroxybutyrate (PHB) is a type of polyhydroxyalkanoate, which is found in various microorganisms and is used in many industries. However, the problem which emerges from the production of PHB is that in in vivo conditions it contains lipids and proteins, which consequently means that organic solvents such as hypochlorite and acetone must be used for lipid removal [10]. Moreover, besides PHA, interest rises for other biodegradable materials. For example, bacterial cellulose can be used in the medical industry as artificial skin or as an aid for wound dressing [11]. As packaging production is concerned, other biopolymers that can be used as a raw material for the production of edible biofilm are agar and inulin, which are also added in food because of their properties to increase textural properties [12]. On the other hand, concerning the anaerobic digestion of some biodegradable materials, there is the possibility that the full biogas potential of biodegradable plastics cannot be achieved in biogas plants because of bioplastics' relatively stable structure [13].

The aim of the study was to produce, analyse, and evaluate the potential for 3D printing with the biopolymers obtained during the treatment of waste brewers' yeast with activated sludge bacteria. The biopolymers that are trying to be extracted include PHA and bacterial cellulose, since it was found after a literature overview that said polymers can be used as a substrate for 3D printing, in order to obtain a material that, due to its biodegradability, can be used in various industries. That way, brewery waste that already requires proper waste management will be used as a cheap substrate for the production of biodegradable polymers, which further emphasizes the concept of a circular economy. After the initial enrichment of active sludge, the cultivation of microorganisms on glucose and organic acids will follow. After that, the cultivation of microorganisms will be performed in a bioreactor with mechanical stirring (SBR). The carbon and nitrogen source, in process in SBR, will be carbohydrates and brewery waste (yeast hydrolysate). Moreover, at the end of the process, the biodegradability of synthesized material will be investigated via biogas potential (BPP) and biomethane potential (BMP). At last, the physical, and mechanical properties of a 3D-printed cube will be tested.

2. Materials and Methods

2.1. Waste Brewers' Yeast

Waste brewers' yeast was acquired at a local large brewery with 1 million hl production annually, mainly of lager beer. Waste brewers' yeast was sedimented after the fermentation

process at said brewery for three days, and was collected, transported to the laboratory, and kept at room temperature (25 °C) until it was used. Characteristics of waste brewers' yeast is shown in Table 1.

2.2. Enrichment of Active Sludge

Enrichment of active sludge was performed by a similar procedure as was described by Li et al. [5]. Wastewater, which contained active sludge from an aerobic tank of local municipal wastewater treatment plant (WWTP), was used as a source of mixed microbial culture. Initial dry biomass matter in said wastewater was 9.70 g/L. 2 L of wastewater, which contained active sludge, was added in each of the two mechanically stirred open reactors (V_{total} = 5 L), and 2 L of water was also added in each reactor in order to reduce biomass concentration. The mixing velocity of the mechanical stirrer was 45 rpm. Aeration was performed by air through diffusers (flow 1 L/min). pH was maintained at 7.0 in both reactors. Enrichment was performed by semi-continuous cultivation. The fresh nutrient medium was pumped via a peristaltic pump (flow 600 µL/min). Composition of nutrient medium was: 1.54 g/L acetic acid, 0.44 g/L propionic acid, 0.17 g/L butyric acid, 0.28 g/L peptone, and 2.10 mL/L salt medium (composition of salt medium 98 mg/L KH_2PO_4, 129 mg/L NH_4Cl, 204 mg/L $MgCl_2$ * $6H_2O$, 42 mg/L $CaCl_2$ * $2H_2O$, 30 mg/L NaOH). Every 24 h, either sludge or water layer was drawn to maintain dry biomass matter at around 2 g/L. Biomass concentration was controlled spectrophotometrically (λ = 600 nm), according to the previously constructed graph ($y = 0.4955x + 0.3799$; $R^2 = 0.9222$). Enrichment of active sludge lasted for four months. This enriched sludge was used as an inoculum for further described experiments. Characteristics of activated sludge is shown in Table 1.

Table 1. Characteristics of waste brewers' yeast and activated sludge.

Characteristics	Waste Brewers' Yeast	Activated Sludge
pH	4.46	6.84
COD (mgO_2/L)	133,670	6800
C/N ratio	61	11

2.3. Cultivation of Mixed Microbial Culture from Enriched Sludge on Glucose and Organic Acids

In each of the three Erlenmeyer flasks, 250 mL of nutrient medium was prepared, which contained glucose (20 g/L), peptone (3 g/L), and KH_2PO_4 (1 g/L). After that, 10 mL of enriched sludge was transferred to each of said Erlenmeyer flasks. Cultivation in each Erlenmeyer flask was conducted for 24 h at room temperature on the magnetic stirrer (200 rpm). After 24 h, content from each Erlenmeyer flask was transferred to three reactors (V_{total} = 5 L), respectively, with mechanical stirring. Each of the three reactors was filled with 4 L of nutrient medium, which contained sugar, peptone, and KH_2PO_4. This phase of the process, where there is no nutrient limitation, is trophophase, and it lasted for a week. At the end of the trophophase, centrifugation (5000 rpm) was performed on the biomass from each of the glass reactors to separate biomass from nutrient media. Separated biomass from each of the glass reactors was transferred into another three glass reactors with mechanical stirring (V_{total} = 5 L) to begin the next phase—idiophase. Then, 4 L of the nutrient medium was added to each of the three reactors. Said nutrient medium contained different organic mixtures (as carbon source) and KH_2PO_4, while peptone (nitrogen source) was omitted. Idiophase lasted for three days. Carbon sources used in different experiments are shown in Table 2.

2.4. Cultivation of Mixed Microbial Culture from Enriched Sludge on Organic Acids

In each of the three Erlenmeyer flasks, 300 mL of enriched sludge was added. Cultivation was conducted for 24 h at room temperature on the magnetic stirrer (200 rpm). After

24 h, content from each Erlenmeyer flask was transferred to three reactors (V_{total} = 5 L), respectively, with mechanical stirring. Each of the three reactors was filled with 4 L of nutrient medium, which contained organic acid(s) 4 g/L, peptone 0.28 g/L, KCl 390 mg/L, NH_4Cl 323 mg/L, KH_2PO_4 89.50 mg/L, and $FeCl_3$ * $6H_2O$ 20 mg/L. This phase of the process, where there is no nutrient limitation is trophophase, and it lasted for a week. At the end of the trophophase, centrifugation (5000 rpm) was performed on the biomass from each of the glass reactors, to separate biomass from nutrient media. Separated biomass from each of the glass reactors was transferred into another three glass reactors with mechanical stirring (V_{total} = 5 L) to begin the next phase—idiophase. The nutrient medium in idiophase for this bioprocess was identical to trophophase nutrient medium, with the exception that nitrogen and phosphorus sources were omitted. pH during trophophase and idiophase was maintained at cca 7.0, while aeration of the reactor was performed by the airflow of 1 L/min. Idiophase lasted for three days. Carbon sources used in different experiments are shown in Table 2.

Table 2. Carbon sources used in different experiments.

24 h Cultivation of Enriched Sludge	Trophophase	Idiophase	Biomass Obtained at the End of the Process (g/L)	Abbreviation
glucose	glucose	propionic acid	1.40	GGP
	glucose	double acid mixture	1.20	GGD
	glucose	triple acid mixture	1.20	GGT
propionic acid	propionic acid	propionic acid	1.00	PPP
	double acid mixture	double acid mixture		PDD
	triple acid mixture	triple acid mixture	0.90	PTT

Double acid mixture: 60% acetic acid + 40% propionic acid. Triple acid mixture: 63% acetic acid + 25% propionic acid + 12% butyric acid.

2.5. Cultivation of Microorganisms from Active Sludge on the Glucose and Brewery Waste

In the Erlenmeyer flask, 250 mL of nutrient medium was prepared, which contained glucose (20 g/L), peptone (3 g/L) and KH_2PO_4 (1 g/L). After that, 10 mL of enriched sludge was transferred to said Erlenmeyer flask. Cultivation in Erlenmeyer flask was conducted for 24 h at room temperature on the magnetic stirrer (200 rpm). After 24 h, content from the Erlenmeyer flask was transferred to a glass reactor (V_{total} = 5 L) with mechanical stirring. The reactor was filled with 4 L of nutrient medium, which contained yeast hydrolysate from the brewery as the sole nutrient source. The concentration of yeast hydrolysate was 70 mL/L. C/N ratio of the yeast hydrolysate was 61. Cultivation of microorganisms from active sludge on the brewery waste lasted for a week.

2.6. Cultivation of Microorganisms from Active Sludge on the Glucose, Propionic Acid, and Brewery Waste

In the Erlenmeyer flask, 250 mL of nutrient medium was prepared which contained glucose (20 g/L), peptone (3 g/L), and KH_2PO_4 (1 g/L). After that, 10 mL of enriched sludge was transferred to said Erlenmeyer flask. In another Erlenmeyer flask, 250 mL of nutrient medium was prepared, which contained propionic acid (20 g/L), peptone (3 g/L), and KH_2PO_4 (1 g/L). After that, 10 mL of enriched sludge was transferred to said Erlenmeyer flask.

Cultivation in both Erlenmeyer flasks was conducted for 24 h at room temperature on the magnetic stirrer (200 rpm). After 24 h, contents from both Erlenmeyer flasks were transferred to the same glass reactor (V_{total} = 5 L) with mechanical stirring. The reactor was filled with 4 L of nutrient medium, which contained yeast hydrolysate from the brewery as the sole nutrient source. The concentration of yeast hydrolysate was 70 mL/L. Cultivation of microorganisms from active sludge on the brewery waste lasted for a week.

2.7. Cultivation of Enriched Sludge on Sucrose and Brewery Waste

After performed cultivations, cultivation on cheap substrates (sucrose and brewery waste) was performed. Firstly, 300 mL of enriched sludge was transferred into 4 L of nutrient medium, which consisted of sucrose 20 g/L, peptone 3 g/L, and KH_2PO_4 1 g/L. Cultivation lasted for 24 h. After 24 h, the whole content was transferred to the SBR reactor (initial working volume $V_{initial}$ = 50 L). The initial nutrient medium in SBR consisted of sucrose 4.50 g/L and brewery yeast hydrolysate 8 mL/L. Cultivation in SBR lasted for 13 days, where for the first 7 days (trophophase) sucrose was used as a carbon source, while brewery yeast hydrolysate was used as a nitrogen source. During the last 6 days (idiophase), sole source of nutrients was sucrose. During trophophase, every day 2 L of fresh nutrient medium (sucrose 4.50 g/L, brewery yeast hydrolysate 8 mL/L) was added to the SBR, while during idiophase, 2 L of the fresh nutrient medium was added every day, in which sucrose was the sole nutrient source (sucrose 4.50 g/L).

2.8. Release of Intracellular Content after Cultivation

Biomass obtained at the end of idiophase in glass reactors was frozen overnight (−18 °C), heat-shocked under a water tap jet (70 °C), and centrifuged (5000 rpm) to break cells and to free intracellular components. The suspension was dried at 50 °C until constant mass. Dried biomass was milled with mortar and pestle and weighed. After that acetone was added in 1:10 ratio. Extraction was performed on the magnetic stirrer (200 rpm) for 24 h. After 24 h 10× volume of ethanol was added. After the organic solvent mixture evaporated, the remaining solid residue was analyzed.

At the end of cultivation in SBR, 25 mL of $FeCl_3$ (30%) was added to better biomass precipitation. Biomass was centrifuged (9000 rpm) for half an hour. The supernatant was decanted, while precipitate was lyophilised and mixed with dichloromethane (1:15 ratio) on the magnetic stirrer for 24 h. The suspension was filtered through filter paper and dried on the rotational evaporator. Decanted supernatant was mixed with acetone, centrifuged, and the precipitate was lyophilised.

2.9. Biodegradability Determination

Biogas (BPP) and biomethane (BMP) potential were determined, according to the method modified by Angelidaki et al. [14].

2.10. 3D Printing

Lyophilised extracted polymer was mixed with a hybrid of acrylic and epoxy resin (manufactured by Allnex, Drogenbos, Belgium) activated by a photo initiator. The ratio of polymer and resin was 30:70. A 3D printer (manufactured by 3DTech, printer in development, Zagreb, Croatia) printed sample of a solid and stable cube (dimensions 20 × 20 × 20 mm).

2.11. Analysis

At the end of all the processes, the following analyses were performed: ATR FT-IR (Perkin Elmer Spectrum 65 FT-IR spectrometer, Markham, ON, Canada), DSC (Mettler Toledo DSC 2 calorimeter, Greifensee, Switzerland), and TGA (Mettler Toledo TGA/DSC 3+, range 40–550 °C, nitrogen 20 mL/min, Greifensee, Switzerland). C/N ratio of yeast hydrolysate was determined via TOC-$L_{CPH/CPN}$ (Shimadzu, Kyoto, Japan). Physical properties of 3D-printed material were determined via a three-point bending test on materials-testing machine Mark-10, considering granulation. Granulations of 100, 50, and 10 µm were tested. Dimensions of 3D printed test plates were 40 × 10 × 1 mm.

3. Results

3.1. Results of Initial Cultivations

FT-IR analysis confirmed the presence of various organic compounds. In every sample, a signal on 3300 cm^{-1} was detected, which is equivalent to N-H, -OH, or a water signal.

Furthermore, signals on 2925, 2850, 1465, 1375, and 750–720 cm^{-1} were detected in each sample, which indicates the aliphatic -CH_2- group. An ester bond was detected in the GGP, GGT, PPP, PDD, and PTT samples, since FT-IR analysis showed the presence of the signal on cca 1740 cm^{-1}. Signals at cca 1650 and 1545 cm^{-1} were also detected on the FT-IR spectra of the GGP, GGD, PPP, and PTT samples (data not shown), which indicates the presence of amid bonds in said samples. Results of FT-IR analysis of extract obtained during initial cultivations are shown in Table 3.

Table 3. Results of FT-IR analysis of extract obtained during initial cultivations.

FT-IR Band (cm^{-1})	Bond Type	Sample
3300	N-H or -OH, water	GGP GGD, GGT, PPP, PDD, PTT
2960, 2870	-CH_3	PDD, PPP, PTT
2925, 2850, 1465, 1375, 750–720	-CH_2- aliphatic	GGP, GGD, GGT, PPP, PDD, PTT
1740	C=O ester	GGP, GGT, PDD, PPP, PTT
1710	C=O acid (dimer)	GGT
1600–1680	C=C aliphatic	GGP, GGT, PPP
1650–1530	N-H, NO_2	GGT, PTT
1490–1530	N-O	GGP, GGT
1460	C-H_3, O-CH_3	PDD, PPP, PTT
1380	CH_3	GGT, PDD, PPP, PTT, GGT
1350–1260, 1100	sec. OH	PDD, PTT
1160	C-O (aliphatic ether)	GGT, PDD, PPP, PTT
1060	C-F, N-N, S=O	PPP, PTT, GGT
700–1000	C-H, C=C	GGP, GGD, GGT, PPP, PDD, PTT

Furthermore, the residue obtained after each extraction was collected, and FT-IR, DSC, and TGA analyses were performed (results shown in Table 4). From the data shown in Table 4, it is visible that the residue of sample PDD after extraction has a signal at 1744 cm^{-1}, which is equivalent to the signal of the C=O ester group. In no other residues was a signal at cca 1740 cm^{-1} detected, which indicates that in the other residues no ester is present. Residues of samples GGD and PPP have signals detected at 1374 and 1398 cm^{-1}, respectively, which was not observed in the other samples. The rest of the detected signals are identical to all the samples. For example, signals at cca 1530 and 1630 cm^{-1} are observed in all the samples and are an indicator of CO and NH bonds, which means that proteins are present in said samples.

Table 4. Results of FT-IR analysis of residue obtained after extraction during initial cultivations.

Residue of Sample	Signal (cm^{-1})
GGP	1027, 1228, 1528, 1630, 1982, 2165, 2925, 3285
GGD	1031, 1228, 1374, 1531, 1627, 2163, 2920, 3271
GGT	1019, 1233, 1531. 1635, 2026, 2167, 2928, 3283
PPP	1031, 1241, 1398, 1543, 1635, 2038, 2163, 2920, 3275
PDD	1031, 1241, 1410, 1559, 1639, 1744, 2026, 2163, 2852, 2920, 3275
PTT	1043, 1241, 1410, 1563, 1639, 2167, 2920, 3287

During DSC analysis of the residues obtained after extraction, loss of mass was noted between 10.4% and 23.1%. Moreover, great losses of mass were observed during the first heating cycles. Crystallization was not detected in any of the samples.

During TGA analysis of the residues obtained after extraction, loss of mass was detected at temperatures higher than 40 °C. Char of all the samples was very stable and did not burn out under ordinary oxidative conditions, which is especially visible in samples GGP and GGD. Ash content in all residue samples varied between 6.5% (GGT) and 25.9% (PDD).

3.2. Cultivation of Active Sludge Bacteria Using Brewery Waste as Nutrient Source

At the end of the cultivation using brewery waste as a nutrient source, FT-IR, DSC, and TGA analysis were performed. During FT-IR analysis of the extract obtained after the bioprocess, where inoculum cultivated on glucose was used as well as microorganisms from active sludge cultivated on the glucose, propionic acid, and brewery waste, a strong signal at 1742 cm^{-1} was observed, which indicates the presence of the C=O group in the esters. Moreover, strong signals at cca 1160, 2853, and 2920 cm^{-1} were detected in both samples. Consequently, it can be concluded that the spectra of both samples are almost identical. However, in the extract obtained after the bioprocess, where inoculum cultivated on glucose was used, a strong signal at 1710 cm^{-1} was detected, which indicates the presence of organic acids.

In the residue obtained after the bioprocess, where inoculum cultivated on glucose was used, a strong signal at 878 cm^{-1} was detected, which was not detected in any other residue samples. In the residue obtained after the bioprocess, where microorganisms from active sludge were cultivated on the glucose, propionic acid and brewery waste were used, a strong signal at 1740 cm^{-1} was detected, which is an indication of ester.

After DSC analysis of the residues after extraction was performed, a loss of mass of 11% was noted. Moreover, no crystallization was detected.

During TG analysis, char content in the samples was 25.9 $\pm$ 2.4%, while ash content was 6 $\pm$ 0.8%. In total, 68 $\pm$ 3.2% of the material was decomposed. During TG analysis of residue obtained after the bioprocess, where inoculum cultivated on glucose was used, peaks at 187.48 and 264.53 °C were observed. The residue obtained after the bioprocess, where microorganisms from active sludge were cultivated on the glucose, propionic acid and brewery waste were used, and a peak at 264.03 °C was observed. A graph of the TG analysis showed thermic stability until 180 and 240 °C, for residues obtained with glucose and microorganisms from active sludge cultivated on the glucose, propionic acid, and brewery waste, respectively. In both samples, linear decline was noted until 550 °C.

3.3. Cultivation of Microorganisms in SBR using Sucrose and Brewing Yeast as Nutrient Source

After cultivation in SBR was performed, gravimetric analysis was conducted, and the total solid concentration was 1.16 g/L. Moreover, the chemical oxygen demand (COD) of the reactor mixture was determined, and it was 11,480 mg O_2/L.

After extraction with dichloromethane was performed, the extract was analyzed with FT-IR (Figure 1). During the cultivation of selected active sludge bacteria using sucrose and brewing yeast hydrolysate as the nutrient source, signals at 1741.3, 1709.6, 1634.3, and 1238 cm^{-1} were detected.

The residue obtained after cultivation in SBR was analyzed by TGA. Loss of mass at 200 °C was 1%, and it progressed linearly. During TGA analysis of the residue, 59.9% of the material was decomposed. Char content in the sample was 16.1%, and ash content was 24%. Higher ash content could be a consequence of $FeCl_3$ addition for the betterment of biomass sedimentation. From the graph shown in the Figure 2, it is clear that the total mass was stable until 50 °C, after which it began to reduce linearly. Linear reduction of total mass was until cca 250 °C, after which reduction was exponential until 550 °C.

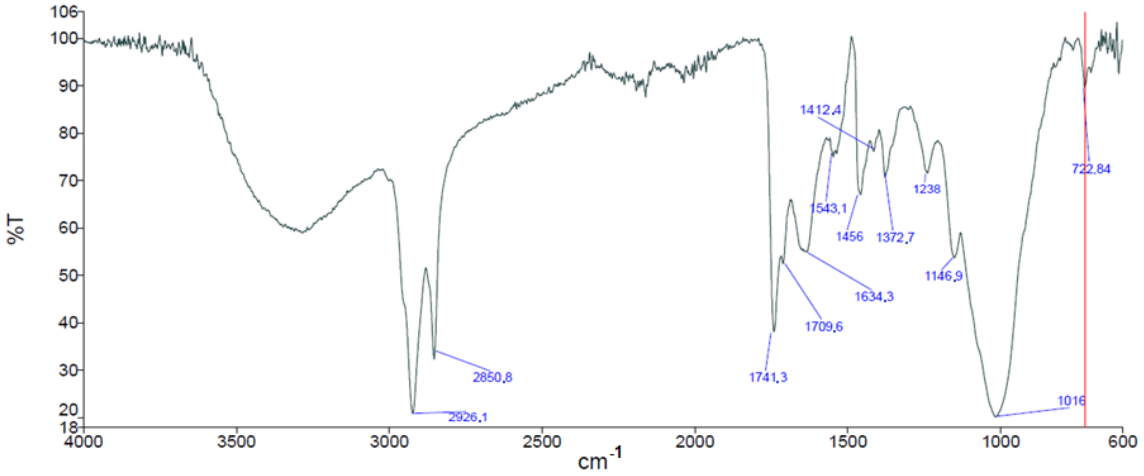

Figure 1. FT-IR spectrum of soluble extract obtained during bioprocess in SBR.

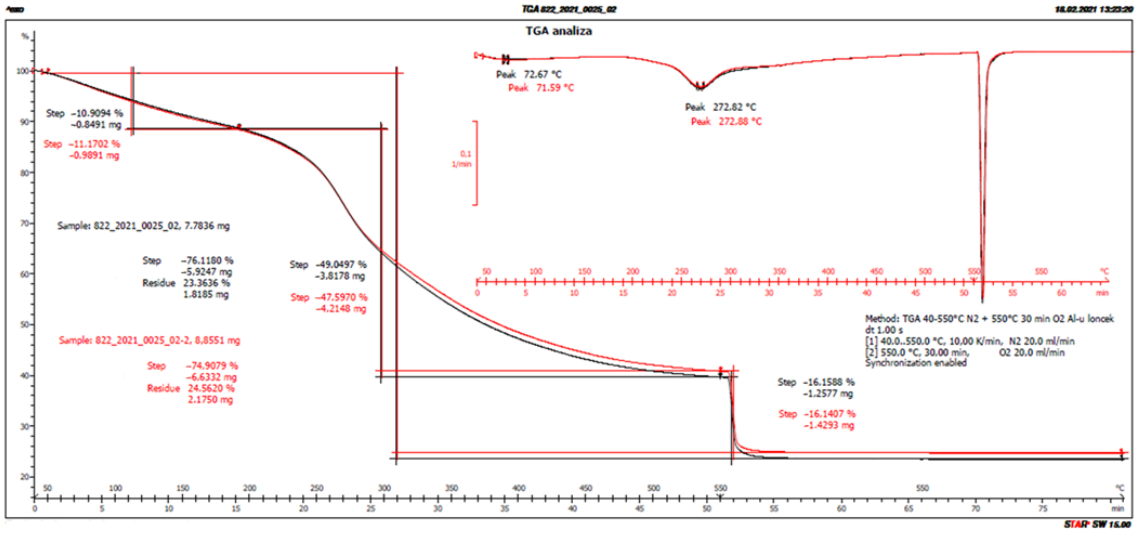

Figure 2. TGA analysis of residue obtained after bioprocess in SBR.

DSC analysis of residue, extract and lyophilized suspended particles in the supernatant were performed. Losses of mass were observed of 20.9%, 20.1%, and 28.7%, respectively. During DSC analysis of the residue and suspended particles in the supernatant, a strong peak at 130 °C was detected, while no peaks were detected during cooling and the second heating. During DSC analysis of extract, several broad transitions during the first scan were noted, while no transition was noted during the second heating scan.

3.4. Biogas Potential of Biomass Obtained after Bioprocess in SBR

Anaerobic digestion of biomass obtained after cultivation in SBR was performed, and results were compared with the biogas/biomethane potential of other microbial biomass found in scientific papers.

From the graph shown in Figure 3, it can be concluded that biogas production in two parallels showed exponential growth during the first five days and reached its maximum at 720 and 600 L/kg$_{COD}$, respectively. The biogas potential of the third parallel showed exponential growth during the first two days, after which linear growth occurred until the 17th day, when a maximum of 550 L/kg$_{COD}$ was achieved.

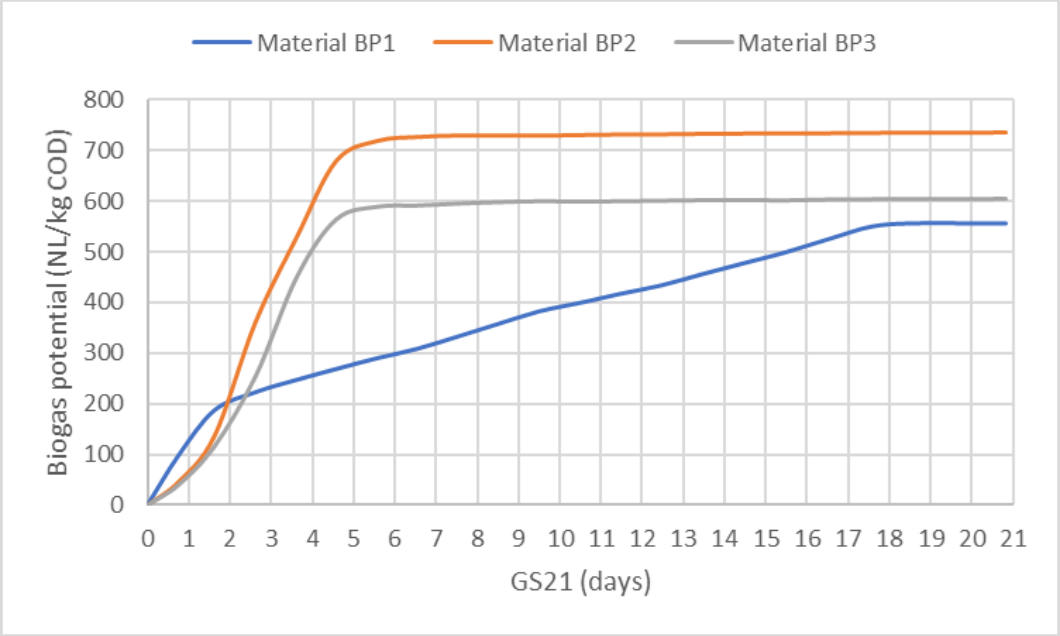

Figure 3. Biogas potential of biomass obtained after bioprocess in SBR.

From the graph shown in Figure 4, it can be concluded that biomethane production in two parallels showed exponential growth during the first five days and reached its maximum at 350 L/kg_{COD}. However, in the third parallel, linear growth of biomethane growth was observed during the first 17 days, after when it also reached its maximum at 350 L/kg_{COD}. It can, thus, be concluded that the third parallel had 8–21% less biogas potential than the first two parallels and that its biogas production was slower. However, the maximal biomethane potential of the third parallel is identical to the maximal biomethane potential of the first two parallels. The biodegradability of three parallels was 97.7%, 98.8%, and 97.0% for 1, 2, and 3, respectively, while the biomethane content was 61.7%, 47.0%, and 56.1% for 1, 2, and 3, respectively.

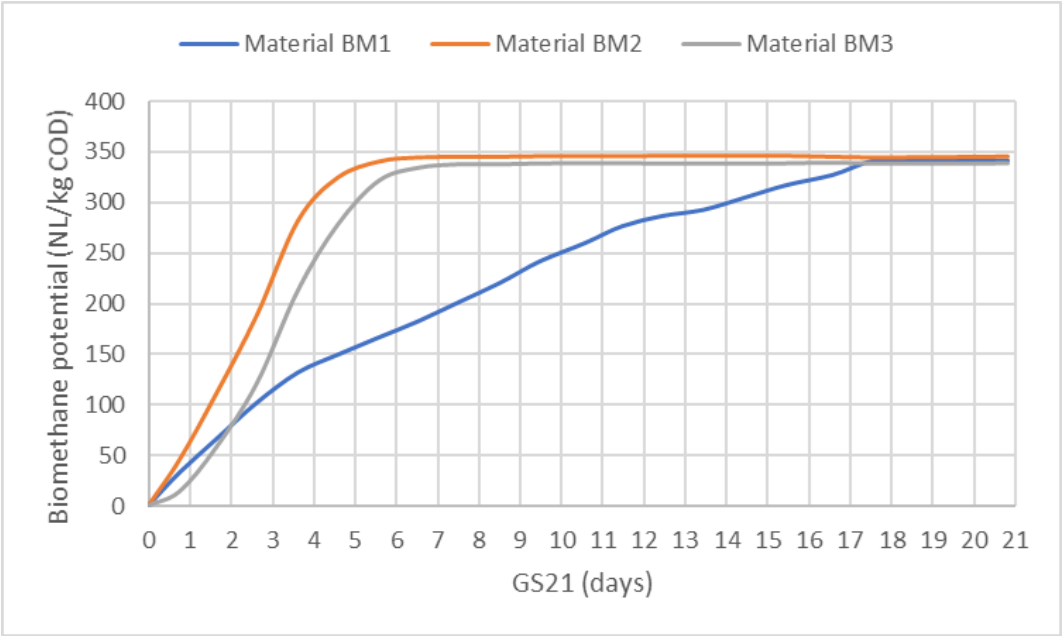

Figure 4. Biomethane potential of biomass obtained after bioprocess in SBR.

3.5. Physical Properties of 3D-Printed Cube Made from Biodegradable Material

After sample preparation and extraction were performed, it was observed that 10.7% of the dry cellular mass obtained after the bioprocess in the SBR was in the form of a suspended, light-colored powder. The material was mixed with a hybrid of acrylic and epoxy resin in various granulations and printed in the form of test plates. The 3D printed test plates made from biodegradable material are shown in Figure 5.

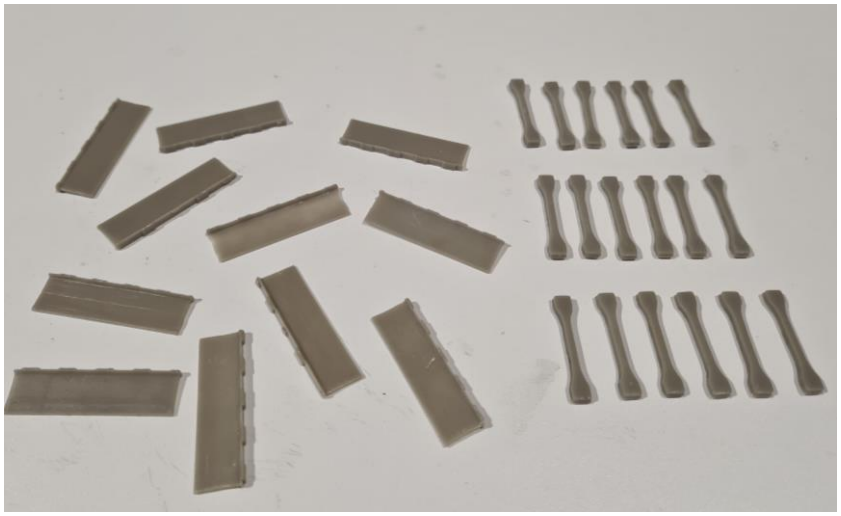

Figure 5. The 3D-printed test plates made from biodegradable material.

The maximum load where breakage of material occurred was tested (data shown in Table 5). The distance at max. load had the highest value (2.82 mm) when a material with granulation of 100 µm was tested, during a max. load of 23.55 N. The lowest value of distance at max. load was 1.74 mm, and it occurred during the testing of a material with granulation of 10 µm and during a max. load of 18.20 N. Moreover, the highest flexural strength was observed during the testing of a material with granulation of 100 µm, while the lowest flexural strength was observed during the testing of a material with granulation of 10 µm.

Table 5. Results of physical properties tests performed on material with various granulation.

Granulation	Max. Load (N)	Distance at Max. Load (mm)	Flexural Strength (MPa)
100 µm	23.55	−2.82	92.42
	24.55	−2.45	
	28.90	−2.26	
50 µm	20.55	−2.32	79.81
	22.32	−2.24	
	23.64	−2.54	
10 µm	17.15	−1.86	60.55
	15.10	−1.79	
	18.20	−1.74	
pure resin	16.25	−1.96	59.53
	16.10	−1.89	
	17.28	−1.84	

From the graph shown in Figure 6, a Young modulus of 3009 N/mm^2 was observed when no biodegradable material was added. The addition of granulated material, which had a diameter of 10 µm, increased the Young modulus to 3230 N/mm^2. When the addition of granulated material with a diameter of 50 µm was tested, it can be observed that the

Young modulus remained approximately the same (3233 N/mm^2), in comparison to the Young modulus of a granulated material with a diameter of 10 µm. When the material with a diameter of 100 µm was tested, an increase in the Young modulus (3549 N/mm^2) was observed.

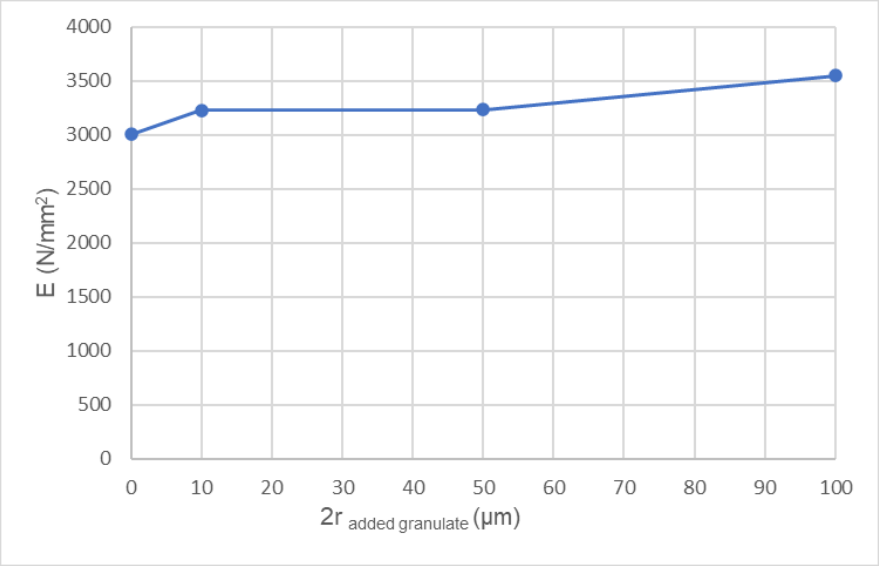

Figure 6. Correlation between Young modulus and granulation of tested material.

After tests of physical properties were performed, it can be concluded that the addition of synthesized biodegradable material increased the Young modulus. Since the mixture obtained after bioprocess is heterogenous, proper testing of the physical properties of each component that build the mixture is limited.

From the graph shown in Figure 7, a bending stress of 59.53 N/mm^2 was observed when no biodegradable material was added. When the material with diameter of 10 µm was added, no significant increase (60.55 N/mm^2) in bending stress was noted. A significant increase in bending stress occurred when a material with a diameter of 50 µm was tested, and the result was 79.81 N/mm^2. The highest value of bending stress was observed when a material with a diameter of 100 µm was tested, and it was 92.42 N/mm^2.

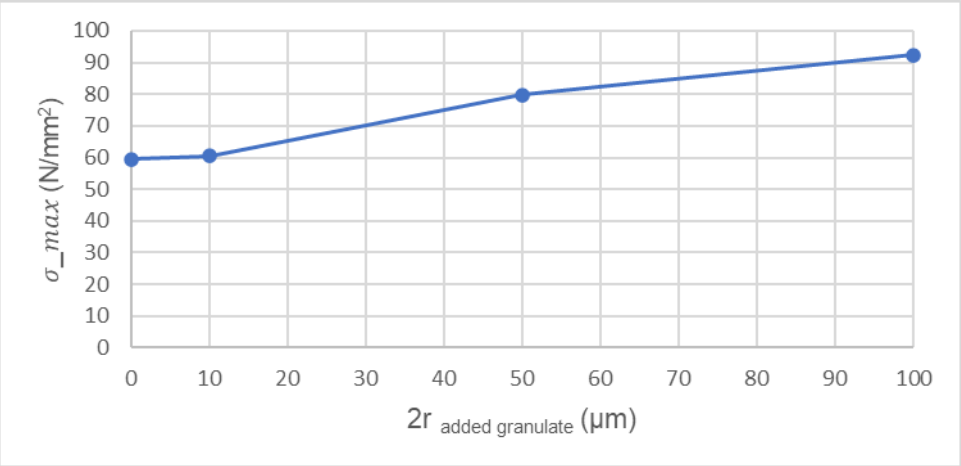

Figure 7. Correlation between bending stress and granulation of tested material.

During testing of the physical properties of a 3D-printed material, Young modulus and bending stress were tested. A 3D-printed cube made from biodegradable material and acrylic resin (shown in Figure 8) was stable and rigid.

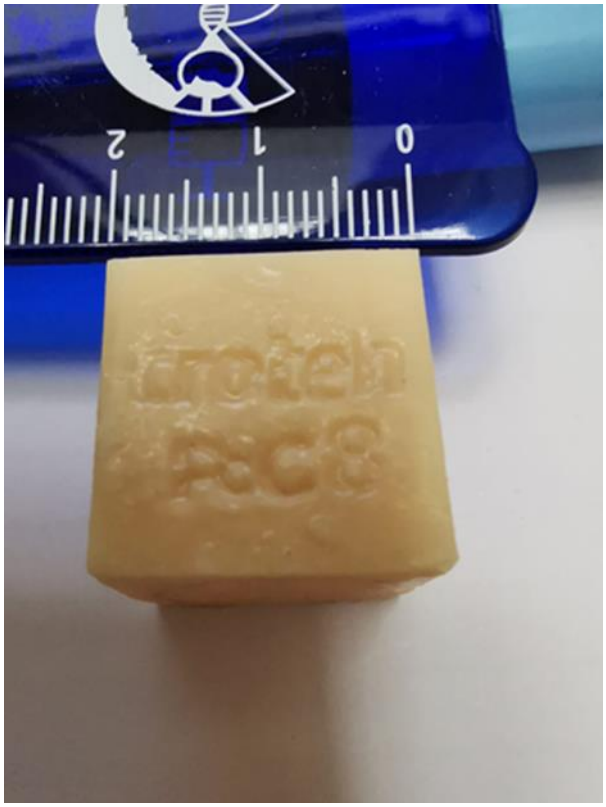

Figure 8. A 3D-printed cube made from biodegradable material.

4. Discussion

Ester bond was detected in the samples GGP, GGT, PPP, PDD, and PTT, since FT-IR analysis showed the presence of the signal on cca. 1740 cm^{-1}. Shapaval et al. [15], in their research, studied the FT-IR spectra of pure components and concluded that a signal in the area of 1715–1700 cm^{-1} indicates the presence of C=O groups of free esters, while a signal in the area of 1800–1715 cm^{-1} indicates the presence of C=O groups of free fatty acids. Nichols et al. [16] performed FT-IR analysis of the following bacteria: *Bacillus subtilis*, *Methylobacterium organophilium*, and *Nitrobacter wynogradskyi*, after which they detected that all three species have a signal at 1740 cm^{-1}, which is equivalent to a carbonyl group. According to the same research, it is observed that pure PHB has a signal at 1752 cm^{-1}. The authors, thus, concluded that the signal shift to 1740 cm^{-1} in the presence of proteins is due to the intermolecular hydrogen bonds between PHB and proteins. Interaction of proteins and PHB was also a part of the study of the research of Isak et al. [17], where it was concluded that the signal at 1654 cm^{-1} and 1540 cm^{-1} is the result of the vibrations and angle stretching of amide bonds. PHB granules in in vivo conditions have an amorphous, non-crystal structure [10]. Signals at cca 1650 and 1545 cm^{-1} are detected on the FT-IR spectra of GGP, GGD, PPP, and PTT samples (data not shown), which indicates the presence of amid bonds in said samples. Furthermore, Forfang et al. [18] conducted a qualitative analysis of lipid extraction from microbial biomass and observed signals at 3010 (=C-H) and 2885, 2925, and 2954 (C-H) as well as 1745 (C=O), 1460 (CH_2), 1070–1250 (C-O-C), and 720 (CH_2) cm^{-1}. Similar signals were observed here, in samples PPP, PDD, and PTT, which can indicate the presence of lipids. Moreover, Auta et al. [19] performed FT-IR analysis of bacterial cellulose, during which they noted signals at 3328 (-OH), 2950 (C-H), 1620 (-OH), and 1153 (asim. C-O-C) cm^{-1}. FT-IR analysis of bacterial cellulose was also conducted by Atykyan et al. [20], during which signals at 3347, 2897, and 1662, between 1000 and 1200 and 847 cm^{-1}, were recorded. Similar signals were detected in some of the tested samples (Table 3), which can indicate the presence of bacterial cellulose.

From the visual examination of samples and results, it is visible that certain limits concern the isolation and purification of specific intracellular biopolymers and cellular components. For example, during PHA extraction, chlorinated solvents are often used, but since it is proven that chlorinated solvents have a negative impact on the environment, eco-friendlier solvents such as acetone are studied as a potential replacement [4]. Due to the aforementioned reason, extraction with acetone was performed, which resulted in the heterogenous mixture that can be confirmed with FT-IR analysis (Table 3).

Crystallization was not detected in any of the samples. Lack of crystallization can be explained because some biopolymers such as PHB in in vivo conditions have an amorphous structure [10].

From the spectrum in the sample obtained after cultivation in SBR, strong signals at 1741.3 and 1709.6 cm^{-1} were detected. Signals in said area could indicate the presence of esters in the sample [15,21]. Furthermore, during FT-IR analysis of PHA produced by *Bacillus subtilis*, Nair et al. [21] detected a signal at 1724 cm^{-1}, which they attributed to stretching of the C=O ester bond, while the signal detected at 1600 cm^{-1} is attributed to stretching of the C=OO bond, and signals at 1228 and 1280 cm^{-1} are attributed to stretching of the C-O-C bond. Moreover, signals at 990 and 1020 cm^{-1} are attributed to the stretching of the C-O-C bond, which is present in extracellular polysaccharides [17]. Signals detected on wavelengths 1721 and 1277 cm^{-1} are an indication of the presence of PHB in the samples [22]. Furthermore, during the cultivation of selected active sludge bacteria, using sucrose and brewing yeast hydrolysate as the nutrient source, signals at 1741.3, 1709.6, 1634.3, and 1238 cm^{-1} were detected.

PHB is a polymer that is, to our knowledge, is most ubiquitous in microorganisms of active sludge. This paper was based on qualitative analysis and was, thus, focused on strictly identifying key organic groups that are of our interest (e.g., ester groups). For example, Nair et al. [21] detected a signal at 1724 cm^{-1} that they attributed to the stretching of the C=O ester bond, while the signal detected at 1600 cm^{-1} is attributed to the stretching of the C=OO bond, and signals at 1228 and 1280 cm^{-1} are attributed to stretching of the C-O-C bond. Signals detected on wavelengths 1721 and 1277 cm^{-1} are an indication of the presence of PHB in the samples [22]. During cultivation in SBR, signals at 1741.3, 1709.6, 1634.3, and 1238 cm^{-1} were detected. Further analyses are needed, but when said results are compared to those of Nair et al. [21] and Trakunjae et al. [22], there is an indication that at least a small amount of PHA is present in the biomass produced in SBR. When studying the FT-IR spectra of cellulose, both Auta et al. [19] and Atykyan et al. [20] observed a signal at around 3300 cm^{-1}, which was not present in the FT-IR spectrum of the sample obtained after cultivation in the SBR.

The residue obtained after cultivation in SBR analyzed by TG showed that loss of mass at 200 °C was 1%, and it progressed linearly. According to the research conducted by Cheng et al. [11], TG analysis of bacterial cellulose was studied, and it was discovered that bacterial cellulose degrades in two stages: at 265 °C and at 445 °C. During TG analysis of pure PHA, the total mass was stable until 237 °C, after which it reduced exponentially until 654 °C, according to Nair et al. [21]. Trakunjae et al. [22] conducted TG analysis of PHB and concluded that PHB degrades rapidly between 240 and 400 °C. TG analysis of bacterial cellulose, performed by Auta et al. [19], has shown that bound water evaporating occurred at 50 °C and degradation after 200 °C. As far as TG analysis of mere *Bacillus* bacterial cells and bacterial spores is concerned, it is known that during the first thermal event loss of mass was between 17.00% and 31.80% and during the second thermal event it was between 31.60% and 38.30%, while during the third thermal event it was between 4.60% and 12.40%, according to Snyder et al. [23]. Trakunjae et al. [22] performed a DSC analysis of pure PHB, which showed that T_m (melting temperature) was 171.8°C, while T_g (glass transition) was 4.03 °C. When DSC analysis of bacterial cellulose was performed by Auta et al. [19], T_g was at 38 °C, while T_m was at 117.31 °C. In comparison to the results presented in this paper, it can be seen that no glass transition was observed, but a strong peak at 130 °C was detected during the analysis of the residue and suspended particles in the supernatant.

When the biogas potential of the biomass obtained after the bioprocess in SBR was tested, the maximum biogas potential of the three parallels was between 550 and 720 L/kg $_{COD}$. However, when biogas production from bacterial cellulose and bioplastics (such as PLA) is discussed, it is noteworthy that in those cases the retention time of the biogas was prolonged to 35 days, while fewer amounts (<50 mL/g_{VS}) of biogas were produced than during the anaerobic digestion of rigid PLA plastic [13]. When the biomethane potential of biomass obtained after bioprocess in SBR was tested, it was observed that a maximum of 350 L/kg_{COD} was achieved. Testing of the biogas potential of various microorganisms was a subject of some studies. For example, research conducted by Gonzalez-Fernandez et al. [24] studied the biomethane potential of microbial algae biomass, and it was discovered that it was between 63.1 and 108.2 mL CH_4/g_{COD}. Besides microalgae, the biomethane potential of other microbial biomass was a subject of extensive studies. For example, Zupančič et al. [25] tested the biomethane potential of wastewater, which contained 3.70% of brewing yeast and a biomethane potential of 0.25 m^3/kg_{COD} was observed. It can, thus, be concluded that microbial biomass obtained after our bioprocess has the highest biomethane potential, in comparison to microalgae and brewing yeast. As a result, hydrolysate of selected bacteria from active sludge is a good substrate for biogas production.

As far as the physical properties of a 3D-printed cube were tested, it can be concluded that the material with granulation of 100 µm showed the highest Young modulus, which was 3.55 GPa. It is known that the Young modulus of pure acrylic resin that was used is about 3.09 GPa, so it can be concluded that the addition of synthesized biodegradable material increased the Young modulus, and, thus, bettered the resin properties. However, heterogeneity of the biodegradable material obtained after the bioprocess complicates detailed analysis of each component present in said material. According to the research conducted by Pinto et al. [26], the Young modulus of pure polylactate was around 3.986 GPa. Moreover, the Young modulus of bacterial cells of *Escherichia coli*, *Bacillus subtilis*, and *Pseudomonas aeruginosa* was studied in research by Tuson et al. [27], and it was observed that the Young modulus was between 50 and 200 MPa, depending on the microbial species.

5. Conclusions

After performing analyses, it can be concluded that the ester bond was present in extracts obtained after cultivation in both a chemically defined (i.e., GGP, GGT, PDD, PPP, PTT) and a complex (sucrose and brewers' yeast) nutrient medium. Furthermore, the use of unfavourable, non-chlorinated extraction solvents contributed to heterogeneous compositions of the samples, which were, thus, challenging to analyse. Therefore, identification, isolation, and purification were demanding to perform, due to the complex structure of both the nutrient medium and the active sludge.

Even though non-chlorinated solvents have certain disadvantages in biopolymer extraction, because of their less hazardous ecological effect, they should be adjusted as a substitute for chlorinated extraction solvents.

The values of the biogas and biomethane potential were as expected, since a maximal biomethane potential of 350 L/kg COD was also achieved. The biodegradability of the biomass was higher than 95%. The obtained biodegradable raw material for 3D printing, when added to the resin, increased the Young modulus of the mixture between 7% and 15% (depending on granulation), in contrast to pure resin.

The use of waste yeast as a substrate for the microbial culture of activated sludge achieved the goal of the research, which is printing a stable and rigid 3D-printed cube made from biodegradable material. However, the results showed that the type of selection of active sludge bacteria makes the process unprofitable, considering the length of the bioprocess and the chemical consumption. Further optimization of the process should focus on more detailed microbial selection as well as biopolymer extraction. In that way, isolation, purification, and identification techniques will be improved, which could achieve higher biopolymer yield.

Author Contributions: Conceptualization and methodology, G.D.Z. and M.P.; validation, G.D.Z. and A.L.; formal analysis and investigation, A.L. and G.D.Z.; writing—original draft preparation, A.L., G.D.Z. and S.B.; writing—review and editing, S.B. and M.P.; supervision, G.D.Z. and M.P.; project administration, M.P. and G.D.Z.; funding acquisition, M.P. and G.D.Z. All authors have read and agreed to the published version of the manuscript.

Funding: This research was co-funded through the state support Program "Proof of Concept" by the Ministry of Economy and Sustainable Development and the HAMAG-BICRO Agency as a part of the project "A process for the production of biodegradable polymer from food industry waste streams as raw material for 3D printing", grant agreement PoC8_8_35.

Institutional Review Board Statement: Not applicable.

Informed Consent Statement: Not applicable.

Data Availability Statement: The datasets generated from this study are available on request to the corresponding author.

Acknowledgments: The authors would like to thank 3DTech for the support in providing the 3D printer and test devices for the analysis of the produced biopolymer.

Conflicts of Interest: Results presented in the paper entitled Biopolymers produced by treating waste brewer's yeast with active sludge bacteria: the qualitative analysis and evaluation of the potential for 3D printing, by authors Gregor D. Zupančič, Anamarija Lončar, Sandra Budžaki, and Mario Panjičko, are the property of Croteh Ltd. (Avenija Dubrovnik 15, 10020 Zagreb). The Faculty of Food Technology, Josip Juraj Strossmayer University of Osijek (Franje Kuhača 18, 31000 Osijek), has no material claims to the results presented in this paper.

References

1. Zeidler, H.; Klemm, D.; Böttger-Hiller, F.; Fritsch, S.; Le Guen, M.J.; Singamneni, S. 3D printing of biodegradable parts using renewable biobased materials. *Procedia Manuf.* **2018**, *21*, 117–124. [CrossRef]
2. Chisenga, S.; Tolesa, G.; Seyoum Workneh, T. Review Article Biodegradable Food Packaging Materials and Prospects of the Fourth Industrial Revolution for Tomato Fruit and Product Handling. *Int. J. Food Sci.* **2020**, *17*, 8879101.
3. Mannina, G.; Presti, D.; Montiel-Jarillo, G.; Suarez-Ojeda, M.-E. Bioplastic recovery from wastewater: A new protocol for polyhydroxyalkanoates (PHA) extraction from mixed microbial cultures. *Bioresour. Technol.* **2019**, *282*, 361–369. [CrossRef]
4. Mohammadi, M.; Hassan, M.; Phang, L.-Y.; Ariffin, H.; Shirai, Y.; Ando, Y. Recovery and purification of intracellular polyhydroxyalkanoates from recombinant Cupriavidus necator using water and ethanol. *Biotechnol. Lett.* **2012**, *34*, 253–259. [CrossRef] [PubMed]
5. Li, H.; Zhang, J.; Shen, L.; Chen, Z.; Zhang, Y.; Zhang, C.; Li, Q.; Wang, Y. Production of polyhydroxyalkanoates by activated sludge: Correlation with extracellular polymeric substances and characteristics of activated sludge. *Chem. Eng. J.* **2019**, *361*, 219–226. [CrossRef]
6. Andreasi Bassi, S.; Boldrin, A.; Frenna, G.; Astrup, F.T. An environmental and economic assessment of bioplastic from urban biowaste. The example of polyhydroxyalkanoate. *Bioresourc. Technol.* **2021**, *327*, 124813. [CrossRef]
7. Martinez-Avila, O.; Llenas, L.; Ponsa, S. Sustainable polyhydroxyalkanoates production via solid-state fermentation: Influence of the operational parameters and scaling up of the process. *Food Bioprod. Process.* **2022**, *132*, 13–22. [CrossRef]
8. Flores-Copa, V.; Romero-Soto, L.; Romero-Calle, D.; Alvarez-Aliaga, M.T.; Orozco-Gutierrez, F.; Vega-Baudrit, J.; Martin, C.; Carrasco, C. Residual Brewing Yeast as Substrate for Co-Production of Cell Biomass and Biofilm Using *Candida maltosa* SM4. *Fermentation* **2021**, *7*, 84. [CrossRef]
9. Ospina-Betancourth, C.; Echeverri, S.; Rodriguez-Gonzalez, C.; Wist, J.; Combariza, M.Y.; Sanabria, J. Enhancement of PHA Production by a Mixed Microbial Culture Using VFA Obtained from the Fermentation of Wastewater from Yeast Industry. *Fermentation* **2022**, *8*, 180. [CrossRef]
10. Kawaguchi, Y.; Doi, Y. Structure of native poly(3-hydroxybutyrate) granules characterized by X-ray diffraction. *FEMS Microbiol. Lett.* **1990**, *70*, 151–156. [CrossRef]
11. Cheng, K.-C.; Catchmark, J.M.; Demirci, A. Enhanced production of bacterial cellulose by using a biofilm reactor and its material property analysis. *J. Biol. Eng.* **2009**, *3*, 12. [CrossRef] [PubMed]
12. Puscaselu, R.; Gutt, G.; Amariei, S. Rethinking the Future of Food Packaging: Biobased Edible Films for Powdered Food and Drinks. *Molecules* **2019**, *24*, 3136. [CrossRef] [PubMed]
13. Shrestha, A.; van-Eerten Jansen, M.C.A.A.; Acharya, B. Biodegradation of Bioplastic Using Anaerobic Digestion at Retention Time as per Industrial Biogas Plant and International Norms. *Sustainability* **2020**, *12*, 4231. [CrossRef]
14. Angelidaki, I.; Alves, M.; Bolzonella, D.; Borzacconi, L.; Campos, J.L.; Guwy, A.J.; Kalyuzhnyi, S.; Jenicek, P.; van Lier, J.B. Defining the biomethane potential (BMP) of solid organic wastes and energy crops: A proposed protocol for batch assays. *Water Sci. Technol.* **2009**, *59*, 927–934. [CrossRef] [PubMed]

15. Shapaval, V.; Brandenburg, J.; Blomqvist, J.; Tafintseva, V.; Passoth, V.; Sandgren, M.; Kohler, A. Biochemical profiling, prediction of total lipid content and fatty acid profile in oleaginous yeasts by FTIR spectroscopy. *Biotechnol. Biofuels.* **2019**, *12*, 140. [CrossRef]
16. Nichols, P.D.; Henson, M.; Guckert, J.B.; Nivens, D.E.; White, D.C. Fourier transform-infrared spectroscopic methods for microbial ecology: Analysis of bacteria, bacteriapolymer mixtures and biofilms. *J. Microbiol. Meth.* **1985**, *4*, 79–94. [CrossRef]
17. Isak, I.; Patel, M.; Riddell, M.; West, M.; Bowers, T.; Wijeyekoon, S.; Lloyd, J. Quantification of polyhydroxyalkanoates in mixed and pure cultures biomass by Fourier transform infrared spectroscopy: Comparison of different approaches. *Lett. Appl. Microbiol.* **2016**, *63*, 139–146. [CrossRef] [PubMed]
18. Forfang, K.; Zimmermann, B.; Kosa, G.; Kohler, A.; Shapaval, V. FTIR Spectroscopy for Evaluation and Monitoring of Lipid Extraction Efficiency for Oleaginous Fungi. *PLoS ONE* **2017**, *12*, e0170611. [CrossRef] [PubMed]
19. Auta, R.; Adamus, G.; Kwiecien, M.; Radecka, I.; Hooley, P. Production and characterization of bacterial cellulose before and after enzymatic hydrolysis. *Afr. J. Biotechnol.* **2017**, *16*, 470–482.
20. Atykyan, N.; Revin, V.; Shutova, V. Raman and FT-IR Spectroscopy investigation the cellulose structural differences from bacteria *Gluconacetobacter sucrofermentans* during the different regimes of cultivation on a molasses media. *AMP Expr.* **2020**, *10*, 84. [CrossRef]
21. Nair, A.M.; Annamalai, K.; Kannan, S.K.; Kuppusamy, S. Characterization of polyhydroxyalkanoates produced by *Bacillus subtilis* isolated from soil samples. *Malaya J. Biosci.* **2014**, *1*, 8–12.
22. Trakunjae, C.; Boondaeng, A.; Apiwatanapiwat, W.; Kosugi, A.; Arai, T.; Sudesh, K.; Vaithanomsat, P. Enhanced polyhydroxybutyrate (PHB) production by newly isolated rare actinomycetes *Rhodococcus* sp. strain BSRT1-1 using response surface methodology. *Sci. Rep.* **2021**, *11*, 1896. [CrossRef] [PubMed]
23. Snyder, A.P.; Tripathi, A.; Dworzanski, J.P.; Maswadeha, W.M.; Wicka, C.H. Characterization of microorganisms by thermogravimetric analysis–mass spectrometry. *Anal. Chim. Acta* **2005**, *536*, 283–293. [CrossRef]
24. Gonzalez-Fernandez, C.; Barreiro-Vescovo, S.; de Godos, I.; Fernandez, M.; Zouhayr, A.; Ballesteros, M. Biochemical methane potential of microalgae biomass using different microbial inocula. *Biotechnol. Biofuels* **2018**, *11*, 184. [CrossRef]
25. Zupančič, G.D.; Škrjanec, I.; Marinšek Logar, R. Anaerobic co-digestion of excess brewery yeast in a granular biomass reactor to enhance the production of biomethane. *Bioresource Technol.* **2012**, *124*, 328–337. [CrossRef] [PubMed]
26. Pinto, V.C.; Ramos, T.; Alves, S.; Xavier, J.; Tavares, P.; Moreira, P.M.G.P.; Guedes, R.M. Comparative failure analysis of PLA, PLA/GNP and PLA/CNTCOOH biodegradable nanocomposites thin films. *Procedia Eng.* **2015**, *114*, 635–642. [CrossRef]
27. Tuson, H.H.; Auer, G.K.; Renner, L.D.; Hasebe, M.; Tropini, C.; Salick, M.; Crone, W.C.; Gopinathan, A.; Huang, K.C.; Weibel, D.B. Measuring the stiffness of bacterial cells from growth rates in hydrogels of tunable elasticity. *Mol. Microbiol.* **2012**, *84*, 874–891. [CrossRef] [PubMed]